C. R. Mecanique 342 (2014) 490–500

Contents lists available at ScienceDirect

Comptes Rendus Mecanique

www.sciencedirect.com

Effect of T-stress on the mode-I fracture toughness of concrete

Yan-hua Zhao *, Bo-han Xu

State Key Laboratory of Coastal and Offshore Engineering, Dalian University of Technology, Dalian 116024, PR China

ARTICLE INFO

Article history:
Received 10 December 2013
Accepted 18 March 2014
Available online 17 June 2014

Keywords:
Fracture mechanics
Concrete
Fracture toughness
T-stress

ABSTRACT

T-stress expressions are provided for three-point bending (TPB) beams and compact tension (CT) specimens and then its influence on mode I fracture toughness of concrete is investigated. The study shows that T-stress is dependent on the specimen's geometry and the material's property as well, and for TPB and CT specimens of regular size, T-stress is so small that its consequences can be neglected. The study also indicates that concrete specimen size should be carefully chosen to make sure the existence of K-dominance ahead of the crack tip, thus fracture toughness extracted from these specimen configurations can be reliable.

1. Introduction

It was once believed that the stress intensity factor (SIF), which describes the singular stress field ahead of a crack tip, was the single controlling parameter for the fracture process in cracked specimens. Nevertheless, further explorations have shown that higher-order terms of the crack tip asymptotic field are also of great importance, especially the second nonsingular term, the so-called T-stress. As the constant term of the Williams series expansion for stress component parallel to the crack flanks [1], T-stress has attracted much attention since it is considered as significantly influencing the stress and strain fields around the crack tip, and thus the fracture failure. When conventional fracture criterions (maximum tangential stress (MTS) criterion) [2], minimum strain energy density criterion (S-criterion) [3], maximum dilatational strain energy criterion (T-criterion) [4], to name but a few are used to predict the onset of fracture, the inclusion of T-stress provides more reliable results [5–7]. For example, when the MTS criterion is used for mode-I fracture without T-stress involvement, the pre-existing crack initiation coincides with the crack plane, as expected. But this is not happening all the time with the presence of T-stress. It was shown in [8] that when T-stress exceeds a certain value, the crack angle will deviate away from the initial crack and the calculated fracture toughness K_{Ic} may decrease a lot. The influence of the T-stress is more notable for brittle materials under mode-II fracture conditions. The fracture angle is no longer $-70°$, as predicted by MTS, and the apparent fracture toughness ratio K_{IIc}/K_{Ic} may be much higher than 0.87 [9], or lower when T-stress is positive. For a general mixed mode fracture, the initiation angle and the effective fracture toughness in the form of $K_{eff} = \sqrt{K_I^2 + K_{II}^2}$ depend on the magnitude and on the sign of T-stress: a negative T-stress makes a smaller angle deviating from the existing crack plane and increases K_{eff}; conversely, a positive T-stress increases the initiation angle and decreases K_{eff}. Besides the initiation angle and fracture toughness, the consequence of T-stress on the crack trajectory has been investigated. For a "double-cleavage drilled compression" specimen, which has a strongly negative T-stress, the crack exhibits a stable fracture

* Corresponding author. Tel.: +8615698891591.
E-mail address: yanhuazh@dlut.edu.cn (Y.-h. Zhao).

http://dx.doi.org/10.1016/j.crme.2014.03.001
1631-0721/

path [10]. For a positive T-stress, however, the crack propagates in the direction away from the line of the initial crack [11]. Considering that T-stress cannot be ignored when the fracture behavior at the crack tip is considered, some researchers even suggest that T-stress, together with SIF, may be used as a two-parameter criterion to predict fracture conditions for mode-I cracks (K_I and T) [12] or a three-parameter criterion for mixed-mode cracks (K_I, K_{II} and T) [13].

In the studies above, the influence of T-stress on the fracture behavior is mostly focused on brittle materials, such as PMMA or brittle rock, or materials with small-to-moderate scale yielding. For concrete material vulnerable to crack, fracture mechanics has found its wide application which could be traced back to 1961 with the works of Kaplan [14]. Nowadays, researches can make a great success in modeling fracture process in bituminous concrete by means of the finite element technique [15]. In concrete fracture mechanics, the reliable determination of fracture toughness is one major task. To the best of our knowledge, no attempt has been made to consider the impact of T-stress when TPB and CT specimens are used to determine concrete fracture toughness. A little doubt remains whether fracture toughness based on those conventional methods is still reliable.

Therefore, the aim of this study is to justify the influence of T-stress term on the fracture toughness (only mode-I fracture is considered in this study) determined from commonly used concrete specimens in laboratory, namely TPB and CT. At the same time, the effect of specimen geometry and material property on the value of T-stress is also investigated.

2. Review of modified MTS criterion for mode I fracture

In this section, the modified MTS criterion proposed in [8] is first briefly reviewed for the reader's convenience, and its application for TPB and CT specimens is investigated in the following sections. For a crack in an isotropic and homogenous solid material subjected to mode-I loading, the tangential stress solution near the crack tip can be written

$$\sigma_{\theta\theta} = \frac{1}{\sqrt{2\pi r}} K_I \cos^3\frac{\theta}{2} + T\sin^2\theta + O\left(r^{1/2}\right) \tag{1}$$

where r and θ are the polar coordinates with the origin located at the crack tip; K_I and T denote the mode I SIF and T-stress, respectively. The higher-order terms $O(r^{1/2})$ can be considered negligible compared to the first and second terms.

According to the MTS [2], the pre-existing crack will grow in the direction along which $\sigma_{\theta\theta}$ at some distance r_c from the crack tip reaches its maximum value. The crack initiation angle θ_0 is determined from $\partial\sigma_{\theta\theta}/\partial\theta = 0$, and by substitution of $\sigma_{\theta\theta}$ from Eq. (1), we get:

$$K_I \sin\theta_0 - \frac{16}{3} T\sqrt{2\pi r_c}\sin\frac{\theta_0}{2}\cos\theta_0 = 0 \tag{2}$$

The onset of fracture occurs when the ($\sigma_{\theta\theta}$) at angle θ_0 from the crack plane and when the distance r_c attains its critical value σ_c. Substitution of $\sigma_{\theta\theta} = \sigma_c$ and $\theta = \theta_0$ into Eq. (1) then yields:

$$\sigma_c\sqrt{2\pi r_c} = K_I\cos^3\frac{\theta_0}{2} + T\sin^2\theta_0\sqrt{2\pi r_c} \tag{3}$$

For pure mode I, i.e., $K_I = K_{Ic}$ and $\theta_0 = 0$, Eq. (3) reduces to:

$$\sigma_c\sqrt{2\pi r_c} = K_{Ic} \tag{4}$$

Here Eq. (4) is particularly addressed, because it is a very important relation to be used in the following analysis.

For convenience, a dimensionless representation is used to include the T-stress's influence

$$B\alpha = \frac{T\sqrt{\pi a}}{K_I}\alpha \tag{5}$$

where $\alpha = \sqrt{2r_c/a}$, a is crack length, and B is stress biaxiality ratio [16] representing the relative magnitude of T-stress to K_I.

Using the conventional MTS criterion, pure mode-I fracture always happens at the angle $\theta_0 = 0$ when the tangential stress $\sigma_{\theta\theta}$ is maximum. But in the presence of T-stress, it occurs only when

$$B\alpha < 0.375 \tag{6}$$

which means that, only under this condition, the second derivative of $\sigma_{\theta\theta}$ at $\theta_0 = 0$ is negative [17].

For $B\alpha > 0.375$, the initial angle deviates from the crack plane, and apparent fracture toughness decreases along with the increase in $B\alpha$. Since our emphasis is restricted to TPB or CT specimens supposed to be under mode-I fracture, i.e., $B\alpha$ at the crack tip should be less than 0.375, readers who are interested in the situation where $B\alpha > 0.375$ can find a more detailed discussion in [17].

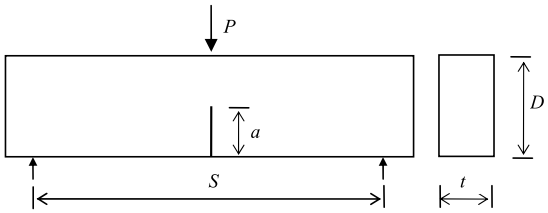

Fig. 1. Three-point bending single-edge notched beam.

3. SIF and *T*-stress for notched TPB specimens

Consider a single edged TPB with span S, depth D, width t and crack length a (cf. Fig. 1). Let β and λ be the crack-to-depth ratio and span-to-depth ratio, respectively:

$$\beta = \frac{a}{D} \qquad \lambda = \frac{S}{D} \tag{7}$$

For a general single edged TPB with λ larger than 2.5, Guinea et al. [18] provided an approximate closed-form expression for K_I according to the principle of superposition

$$K_I = \sigma\sqrt{D}k_\lambda(\beta) \quad \text{with } \sigma = \frac{6M}{tD^2} \tag{8}$$

where M is the bending moment in the central cross-section, and in case of TPB $M = \frac{1}{4}PS$; $k_\lambda(\beta)$ is a dimensionless shape function of the form:

$$\begin{aligned} k_\lambda(\beta) &= \frac{\beta^{1/2}p_\lambda(\beta)}{(1-\beta)^{2/3}(1+3\beta)} \\ &= \frac{\beta^{1/2}}{(1-\beta)^{2/3}(1+3\beta)}\left\{p_\infty(\beta) + \frac{4}{\lambda}\left[p_4(\beta) - p_\infty(\beta)\right]\right\} \end{aligned} \tag{9}$$

where $p_\lambda(\beta)$ is a combination of shape functions of $p_4(\beta)$ ($\lambda = 4$ for standard TPB) and $p_\infty(\beta)$ ($\lambda = \infty$ for pure bending); $p_4(\beta)$ and $p_\infty(\beta)$ are determined to be cubic polynomials by means of curve fitting technique:

$$p_4(\beta) = 1.9 + 0.41\beta + 0.51\beta^2 - 0.17\beta^3 \tag{10a}$$

$$p_\infty(\beta) = 1.99 + 0.83\beta - 0.31\beta^2 + 0.41\beta^3 \tag{10b}$$

Eqs. (8)–(10) are valid for any β varying between 0 and 1, and for any $\lambda \geq 2.5$. The SIF solution for TPB is ready now, even though the T-stress expression is not available in the literature. Leevers and Radon [16] provided some numerical results of B for standard TPB; however, studies on the higher order terms of the crack tip asymptotic field [19] using a hybrid crack element show that the estimate in [16] seems unsatisfactory for the TPB. Besides, the general expression of T-stress for TPB [19] is only limited to the case in which β varies from 0.05 to 0.6.

In [18], the authors proposed a general expression for the SIF of TPB with span-to-depth ratio $\lambda \geq 2.5$, where the SIF was decomposed into the sum of SIF caused by pure bending and a standard TPB according to the Saint-Venant's principle. As two terms of stress component at the crack tip, the principle of superposition is applicable to T-stress. Following the same procedure for SIF deduction in [18], T-stress for any span-to-depth ratio $\lambda \geq 2.5$ can be sought in the form

$$\left(\frac{T}{\sigma}\right)_\lambda = \left(\frac{T}{\sigma}\right)_\infty - \frac{4}{\lambda}\left[\left(\frac{T}{\sigma}\right)_\infty - \left(\frac{T}{\sigma}\right)_4\right] \tag{11}$$

where σ has the exactly same meaning as in Eq. (8); $(\frac{T}{\sigma})_\infty$ and $(\frac{T}{\sigma})_4$ represent dimensionless T-stresses for bending and standard TPB specimens, respectively, and numerical computations with finite element program package Abaqus have led to the following expressions using a fitting procedure:

$$\left(\frac{T}{\sigma}\right)_4 = \frac{0.9582\beta^3 - 2.1562\beta^2 + 1.8127\beta - 0.4405}{(1-\beta)^2} = \frac{q_4(\beta)}{(1-\beta)^2} \tag{12a}$$

$$\left(\frac{T}{\sigma}\right)_\infty = \frac{0.9012\beta^3 - 2.438\beta^2 + 2.1988\beta - 0.5034}{(1-\beta)^2} = \frac{q_\infty(\beta)}{(1-\beta)^2} \tag{12b}$$

The equation above is valid for a general range of β values ($0 < \beta < 1$) with a coefficient of determination R^2 for each curve close to 1.

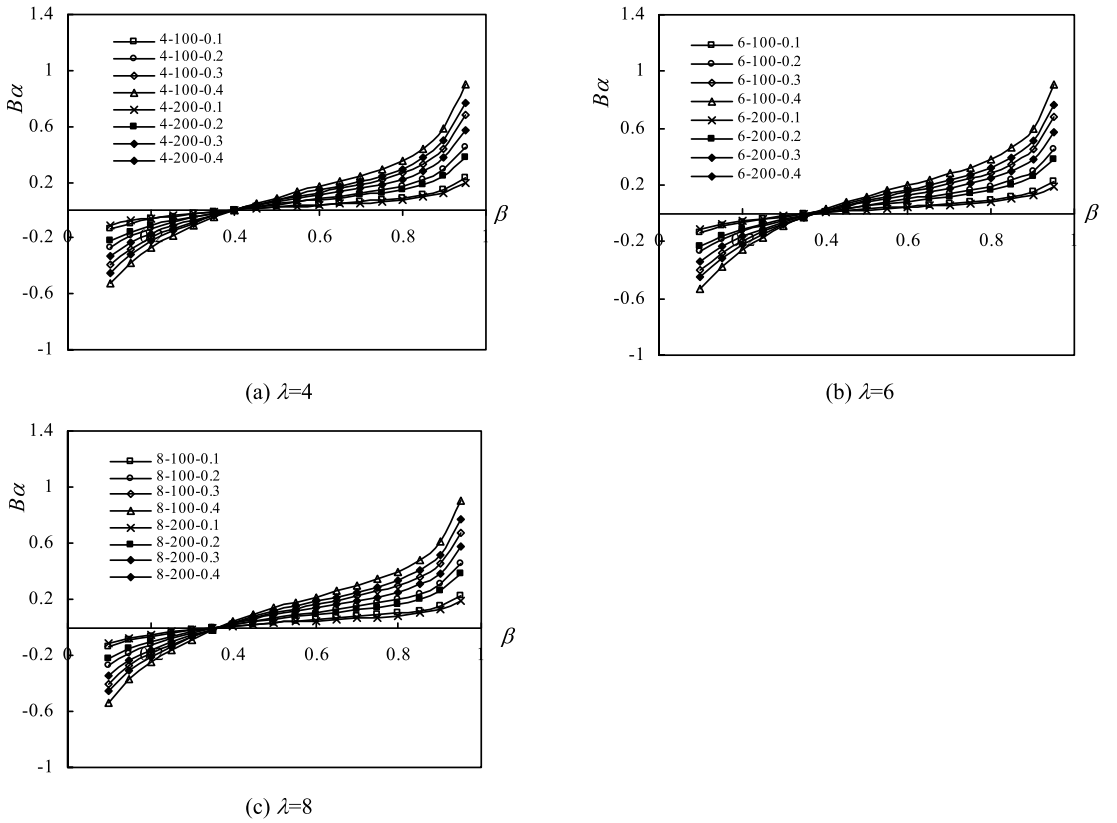

(a) λ=4 (b) λ=6

(c) λ=8

Fig. 2. Theoretical predictions of $B\alpha$ for different D and K_{Ic}/f_t.

Normalizing T-stress in Eq. (11) against SIF in Eq. (8) and multiplying by $\alpha = \sqrt{2r_c/a}$ lead to the $B\alpha$ for TPB specimens:

$$B\alpha = \frac{q_\infty(\beta) - \frac{4}{\lambda}[q_\infty(\beta) - q_4(\beta)]}{p_\infty(\beta) - \frac{4}{\lambda}[p_\infty(\beta) - p_4(\beta)]}\sqrt{\frac{\pi}{1-\beta}}(1+3\beta)\sqrt{\frac{2r_c}{a}} \tag{13}$$

r_c, representing a critical distance where the fracture actually happens, is assumed to be a material property. Since the value of r_c is not easy to verify directly, we used the method suggested by [20], similar to the maximum normal stress criterion [21], that is, σ_c in Eq. (4) takes the value of the material tensile strength, while for TPBs, the tensile strength should take the flexure tensile strength f_r rather than the uniaxial tensile strength f_t, so that we utilized an empirical relationship expression between these two variables which was proposed in [22]:

$$f_r = \gamma f_t = \left(1 + \frac{49.25}{D}\right) f_t \tag{14}$$

where D (mm) is the depth of the TPB. Thus r_c is estimated by:

$$r_c = \frac{1}{2\pi}\left(\frac{K_{Ic}}{f_r}\right)^2 = \frac{1}{2\pi}\left(\frac{K_{Ic}}{\gamma f_t}\right)^2 \tag{15}$$

Substitution of Eq. (15) into Eq. (13) gives:

$$B\alpha = \frac{q_\infty(\beta) - \frac{4}{\lambda}[q_\infty(\beta) - q_4(\beta)]}{p_\infty(\beta) - \frac{4}{\lambda}[p_\infty(\beta) - p_4(\beta)]}\sqrt{\frac{1}{\beta-\beta^2}}(1+3\beta)\sqrt{\frac{1}{D}}\frac{K_{Ic}}{\gamma f_t} \tag{16}$$

Eq. (16) is valid for any $\lambda \geq 2.5$ and any β will be welcome. Referring to Eq. (16), we can conclude that $B\alpha$ at the crack tip of TPB specimens depends not only on the specimen geometry, but also on the material's properties. Figs. 2–3 report $B\alpha$ values versus $\beta = a/D$ for different values of D, λ and K_{Ic}/f_t. $D = 100$ mm, 200 mm, $\lambda = 4, 6, 8$ and $K_{Ic}/f_t = 0.1, 0.2, 0.3, 0.4$ are taken for consideration since these are in the geometrical and material parameter ranges generally used in the laboratory.

With reference to Figs. 2–3, the following conclusions can be drawn:

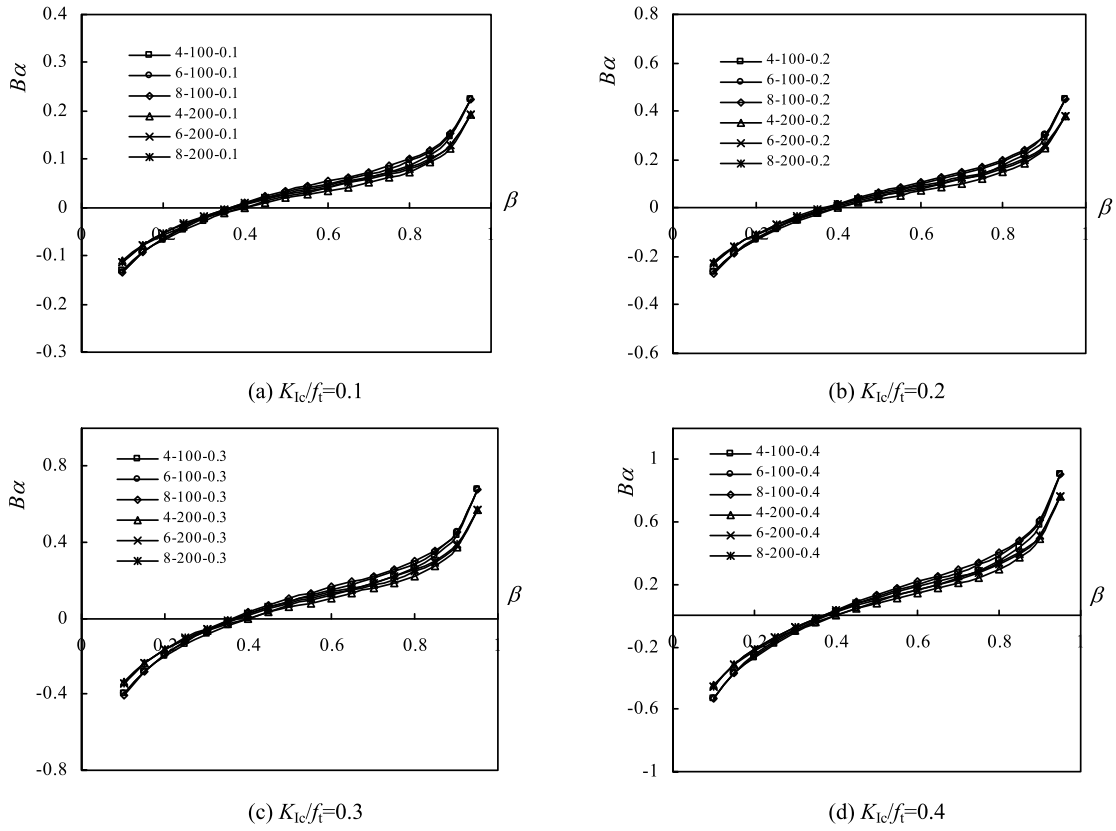

Fig. 3. Theoretical predictions of $B\alpha$ for different D and λ.

(1) in all, $B\alpha$ (normalized T-stress effect) increases when increasing the relative crack length β whatever the values of D, λ and K_{Ic}/f_t are actually. T-stress is negative when $\beta < 0.4$ (approximately), and positive for $\beta > 0.4$. For $\beta = 0.4$, T-stress has its minimum value (near to zero). According to the modified MTS criterion, non-positive T-stress will definitely have no contribution to crack initiation under mode-I fracture conditions;
(2) as shown from Figs. 2a–c, larger D results in smaller $B\alpha$ in absolute value form for the same λ and K_{Ic}/f_t, while for the same values of λ and D, the absolute value of the T-stress becomes greater as K_{Ic}/f_t increases;
(3) Figs. 3a–c depict the influence of λ on the distribution of T-stress, and it is clear that for TPB specimens, T-stress is not as sensitive to λ as it is to D and K_{Ic}/f_t.

When SIF is used to characterize the fracture behavior, we must bear in mind that singular stress field should be dominant near the crack tip. That is to say, linear elastic fracture mechanics (LFFM) is valid only in the K-dominance zone. It is commonly accepted that when the distance from the crack tip is less than $1/25a$, then the region within this distance is dominated by the singular term K. This is the reason why ASTM specifies the specimen size for testing fracture toughness of metallic materials [23]. The same thing can be said for r_c introduced in the MTS criterion or modified MTS criterion. That is, r_c used in TPB specimens, is required to follow:

$$a \geq 25r_c = 25 \cdot \frac{1}{2\pi}\left(\frac{K_{Ic}}{\gamma f_t}\right)^2 \tag{17}$$

It is noteworthy to highlight that the modified MTS is applicable in the limit of linear elastic materials. It fails to be utilized in concrete fracture directly, since concrete follows an obvious non-linearity fracture behavior due to the presence of a fracture process zone (FPZ) ahead of the macroscopic crack, which includes initial crack length a_0 and extended crack length Δa [24]. Nevertheless, when the concept of equivalent crack length a_e is adopted during crack propagation instead of a_0, the crack problem at the tip of a_e can be treated using LEFM. This method is widely adopted in concrete fracture models, such as the two-parameter fracture model (TPFM) [25], the effective crack model [26] (ECM), and the double-K fracture model [27] (DKFM), and so on. Recently, the method of equivalent elastic crack is used in [24] to interpret the size effect of concrete fracture toughness. Besides, the equivalent crack concept has found its application in wood fracture [28,29]. Fortunately, the equivalent crack concept does not exclude cohesive forces. On the contrary, the cohesive force acting on the FPZ is taken into account in DKFM to explain the crack resistance mechanism.

In most cases, the ultimate limit state of concrete members is what we are interested in, so fracture toughness is often used to denote that unstable fracture state, such as K_{Ic}^{s} in TPFM and K_{Ic}^{un} in DKFM. Some researchers, however, suggested that the initiation of the first crack extension deserves much more attention, since it is believed to be an important material property [30–32]. Correspondingly, the initial cracking toughness K_{Ic}^{ini} was introduced in DKFM and recently included in the 2005 Norm for Fracture Test of Hydraulic Concrete in China (DL/T 5332-2005) [33]. Now robin tests are being carried out and discussed for RILEM recommendation test method of double-K fracture toughness in DKFM. K_{Ic}^{ini}, marking the crack propagation state change from elastic-linear to nonlinear, can be directly determined using LEFM. Similarly, K_{Ic}^{s} and K_{Ic}^{un} can also be experimentally determined using LEFM based on the equivalent crack concept. When those fracture parameters for mode-I fracture of concrete are determined, however, no consideration is given to the existence of T-stress. Next we use some experimental data to discuss the effect of T-stress on fracture toughness of concrete based on the modified MTS criterion.

As described in Eq. (17), r_c introduced in the modified MTS criterion should be kept small to ensure K-dominance zone at the crack tip. Specifically, when K_{Ic}^{ini} of concrete is determined experimentally, pre-notch length a_0 should be carefully chosen to follow Eq. (17) where a is replaced by a_0, and K_{Ic} by K_{Ic}^{ini}. Likewise, for the critical unstable state, the external load and the cohesive force can be superimposed to the linear elastic filed ahead of the critical equivalent crack length a_c. Thus a_c must meet

$$a_c \geq 25 \cdot \frac{1}{2\pi}\left(\frac{K_{Ic}^{un} - K_{Ic}^{c}}{\gamma f_t}\right)^2 \tag{18}$$

where K_{Ic}^{c} is the fracture toughness caused by the cohesive force acting along the FPZ. According to three-parameter law in the DKFM [34], i.e. $K_{Ic}^{un} - K_{Ic}^{c} = K_{Ic}^{ini}$, Eq. (18) can be rewritten as:

$$a_c \geq 25 \cdot \frac{1}{2\pi}\left(\frac{K_{Ic}^{ini}}{\gamma f_t}\right)^2 \tag{19}$$

Considering the fact that the critical equivalent crack length a_c is usually larger than a_0, Eq. (19) follows naturally once a_0 meets the requirements of Eq. (17). In a word, one must be careful in the choice of the pre-notch length for the sake of the K-dominance zone ahead of the crack. Many researchers, however, often miss this point, which will be demonstrated in the following example.

Another idea behind the equivalent crack concept is that the concrete specimen is supposed to be sufficient large, usually at least three times the maximum size of the coarse aggregate, so that concrete can be treated as homogenous macroscopically, which is one of the basic assumptions of LEFM. For notched specimens, the uncracked ligament (D–a_0 and D–a_c) needs to be at least three times the maximum aggregate to assure that concrete is macroscopically homogeneous and continuous.

Next some experimental results reported in [34–36] are utilized to substantiate the validity of fracture toughness in the TPFM and DKFM based on the modified MTS criterion. Table 1 lists the relevant calculation results.

(1) In TPFM, TPBs with different depth D are selected for analysis. Since no initial cracking toughness K_{Ic}^{ini} is available, the mean value from those concrete specimens (A1, A2, A3 and A4 from Table 1) exhibiting an almost same tensile strength is borrowed. From columns ⑬ and ⑭, it can been seen that for large and medium-size specimens CL1, CL2, CM1 and CM2, a_0 and a_c can satisfy Eq. (17), and the uncracked size in terms of D–a_0 and D–a_c is larger than three times d_a simultaneously. This means in these four specimens, the K-dominance zone exists at the crack tip. Further investigation evidence that both $B\alpha_0$ and $B\alpha_c$ are negative; thus T-stress has no effect on the determination of fracture toughness based on Eq. (6). In other words, fracture toughness values determined from these four specimens are reliable. In contrast, specimens CS1, CS2, CS3 and CS4 having smaller a_0 fail to follow Eq. (17). More importantly, the ligament length D–a_c is too small (less than three times the maximum size of aggregate d_a) to guarantee the homogeneity ahead of the crack, which is the basic assumption of LEFM. In turn, fracture toughness values determined from these four specimens remain questionable.

(2) Series B and C are two sets of TPBs with similar strength and initial crack length but different D only. Series B has smaller D ($D = 203$ mm), failing to meet the requirements for LEFM application demonstrated by Eq. (17); thus fracture toughness from series B makes no sense. For series C with larger specimen size ($D = 305$ mm), a_0 and a_c are far larger than r_c, thus guarantying the K-dominance region valid at r_c. Also, the uncracked ligament lengths D–$a_0 = 130.84$ mm and D–$a_c = 107.36$ mm are both larger than $3d_a = 57$ mm for series C. The T-stress for series C has values $Ba_0 = 0.053$ and $Ba_c = 0.075$, both smaller than 0.375, which means that there is no influence on double-K fracture parameters. In summary, double-K fracture toughness values from series C are valid.

(3) In DKFM, four other kinds of specimen with different span-to-depth ratio $\lambda = 3, 4, 5, 6$ are used for discussion. Table 1 reveals that the pre-notch length a_0 of all specimens in this set meets the requirement represented by Eq. (17), and uncracked ligament lengths D–a_0 and D–a_c for all the specimens used are larger than $3d_a = 60$ mm. Furthermore, it is found from columns ⑩ and ⑪ that T-stress values for this specimen set are less than 0.375, implying no effect on the values of double-K fracture parameters. In conclusion, fracture toughness determined from this specimen set is reliable.

Table 1
T-stress evaluations at the crack tip for TPB specimens.

	Spe. No.	λ	D (mm)	d_a (mm)	(f_t) (MPa)	γ	K_{Ic}^{ini} (MPa m$^{1/2}$)	K_{Ic}^{ini}/f_t (m$^{1/2}$)	β_0	β_c	$B\alpha_0$	$B\alpha_c$	r_c (mm)	$25r_c$ (mm)	a_0 (mm)	$D-a_0$ (mm)	$D-a_c$ (mm)
		①	②	③[a]	④[b]	⑤	⑥	⑦	⑧	⑨	⑩	⑪	⑫	⑬	⑭	⑮	⑯
TPFM [35]	CL1	4	225	19	2.50	1.219	0.324[c]	0.130	0.333	0.348	−0.018	−0.014	1.80	44.90	74.93	150.07	146.70
	CL2		225			1.219		0.130	0.333	0.386	−0.018	−0.003	1.80	44.90	74.93	150.07	138.15
	CM1		150			1.328		0.130	0.318	0.379	−0.026	−0.006	1.52	37.89	47.70	102.30	93.15
	CM2		150			1.328		0.130	0.324	0.509	−0.024	0.029	1.52	37.89	48.60	101.40	73.65
	CS1		75			1.657		0.130	0.293	0.497	−0.040	0.029	0.97	**24.37**	**21.98**	**53.02**	**37.73**
	CS2		75			1.657		0.130	0.293	0.547	−0.040	0.042	0.97	**24.37**	**21.98**	**53.02**	**33.98**
	CS3		75			1.657		0.130	0.293	0.533	−0.040	0.039	0.97	**24.37**	**21.98**	**53.02**	**35.03**
	CS4		75			1.657		0.130	0.293	0.530	−0.040	0.038	0.97	**24.37**	**21.98**	**53.02**	**35.25**
DKFM [34]	Series B	3.75	203	19	4.24	1.243	0.843	0.232	0.616	0.684	0.083	0.109	5.54	**138.40**	**125.05**	**77.95**	**64.15**
	Series C		305		4.31	1.161	0.778	0.212	0.571	0.648	0.053	0.075	5.28	132.09	174.16	130.84	107.36
DKFM [36]	A1	3	200	20	2.58	1.246	0.298	0.116	0.300	0.405	−0.032	−0.005	1.36	34.08	60.00	140	119.00
	A2	4				1.246	0.316	0.122	0.300	0.389	−0.029	−0.002	1.53	38.32	60.00	140	122.20
	A3	5				1.246	0.332	0.129	0.300	0.386	−0.027	0.001	1.69	42.30	60.00	140	122.80
	A4	6				1.246	0.351	0.136	0.300	0.368	−0.027	−0.002	1.89	47.28	60.00	140	126.40

[a] d_a represents the maximum size of aggregates;
[b] $f_t = 0.4983\sqrt{f_c'}$ if no tensile strength is available, where f_c' is the cylinder compressive strength;
[c] The average of A1, A2, A3 and A4 for their almost equal tensile strength.

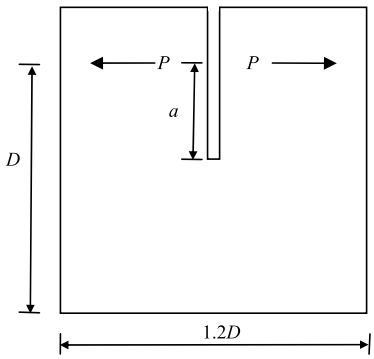

Fig. 4. Notched compact tension specimen.

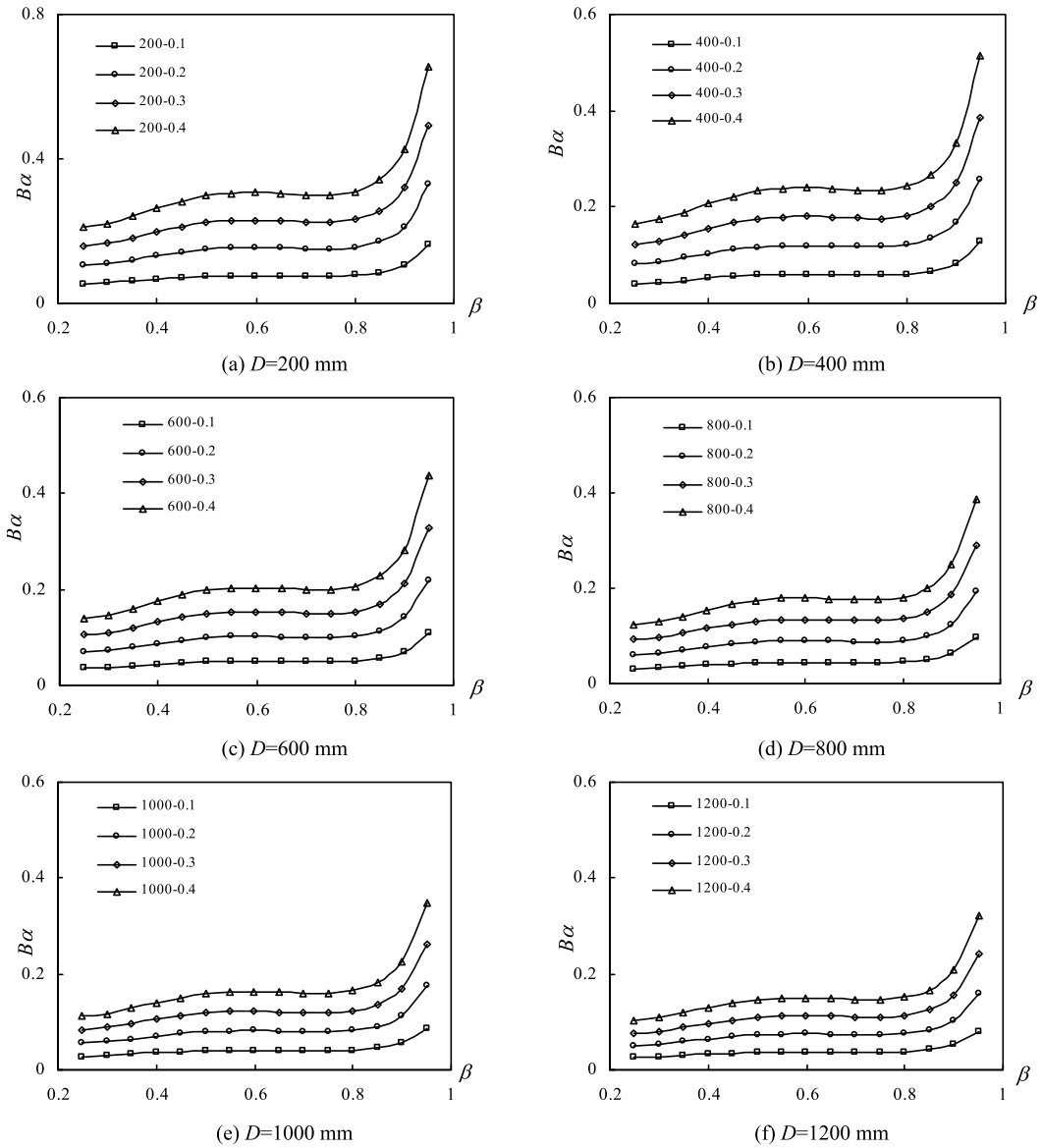

Fig. 5. Theoretical predictions of $B\alpha$ for different K_{Ic}/f_t.

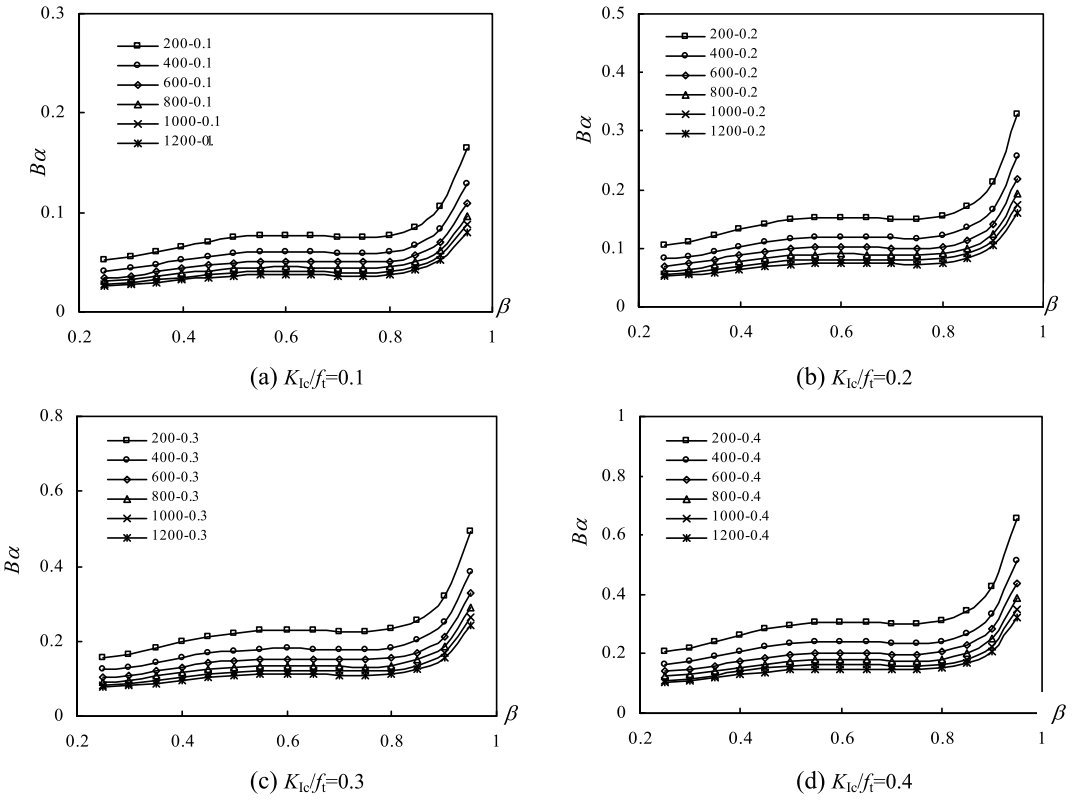

Fig. 6. Theoretical predictions of $B\alpha$ for different D.

4. *T*-stress for notched CT specimens

For the standard CT specimen (cf. Fig. 4) recommended by ASTM [23], the value of $B\alpha$ at the crack tip can be calculated following the same procedure as in the case of the TPB specimen, and the final form is given by data curve fitting [37]:

$$B\alpha \cong \frac{0.7702 - 6.572\beta + 26.665\beta^2 - 43.446\beta^3 + 29.695\beta^4 - 6.6886\beta^5}{\sqrt{1-\beta}}\sqrt{\frac{2r_c}{a}} = \frac{0.7702 - 6.572\beta + 26.665\beta^2 - 43.446\beta^3 + 29.695\beta^4 - 6.6886\beta^5}{\sqrt{\beta-\beta^2}}\sqrt{\frac{1}{\pi D}}\frac{K_{Ic}}{\gamma f_t} \tag{20}$$

The above solution is recommended for cracks with $\beta > 0.25$.

Figs. 5–6 show the variation of $B\alpha$ with β as predicted by Eq. (20), where the specimen's size D is practically between 200 and 1200 mm, and where K_{Ic}/f_t ranges from 0.1 to 0.4. Compared to TPB specimens, the T-stress for notched CT specimens has its own characteristics.

(1) $B\alpha$ increases monotonically when the crack length grows for small β values, and reaches its first peak value approximately at $\beta = 0.6$; then $B\alpha$ drops a little before increasing dramatically. In addition, the $B\alpha$ value is always positive, which is very different from the TPB case.
(2) For the same D value, the $B\alpha$ values increase with K_{Ic}/f_t, a trend similar to the case of TPB specimens.
(3) For the same value of K_{Ic}/f_t, a larger D value results in a smaller value of $B\alpha$. And it is interesting to notice that, for $D \geq 800$ mm, no large difference is observed in the T-stress distribution.

Next the experimental data obtained on CT specimens in [38] are examined to verify the effect of T-stress on fracture toughness. All the specimens have a relative initial crack length $a_0/D = 0.4$ and maximum aggregate size $d_a = 25$ mm. In addition, the tensile strength is reported to be 5.21 MPa. The computed results are tabulated in Table 2. It is clear that all the specimens can satisfy the condition denoted by Eq. (17), and the values of the uncracked ligament length in terms of D–a_0 and D–a_c are all larger than $3d_a = 75$ mm. Moreover, Table 2 also shows that for laboratory-size CT specimens, the T-stress value at the crack tip is not high enough to affect the crack tip, i.e., $B\alpha < 0.375$, which means that mode-I fracture can be guaranteed to happen, and that the apparent fracture toughness thus determined is the true fracture toughness.

Table 2
T-stress evaluations at the crack tip for CT specimens.

D (mm) ①	γ ②	K_{Ic}^{ini} (MPa m$^{1/2}$) ③	K_{Ic}^{ini}/f_t ④	β_c ⑤	$B\alpha_0$ ⑥	$B\alpha_c$ ⑦	r_c (mm) ⑧	$25r_c$ (mm) ⑨	a_0 (mm) ⑩	$D-a_0$ (mm) ⑪	$D-a_c$ (mm) ⑫
200	1.246	0.635	0.122	0.602	0.080	0.093	1.52	38.06	80	120	79.6
		0.656	0.126	0.565	0.083	0.096	1.62	40.61			87
		0.662	0.127	0.601	0.084	0.097	1.65	41.36			79.8
		0.753	0.145	0.62	0.095	0.110	2.14	53.51			76
		0.725	0.139	0.603	0.092	0.106	1.98	49.61			79.4
300	1.164	0.675	0.130	0.563	0.075	0.086	1.97	49.28	120	180	131.1
		0.711	0.136	0.568	0.079	0.091	2.19	54.68			129.6
		0.456	0.088	0.632	0.050	0.058	0.90	22.49			110.4
		0.740	0.142	0.535	0.082	0.094	2.37	59.23			139.5
		0.614	0.118	0.615	0.068	0.079	1.63	40.77			115.5
400	1.123	0.562	0.108	0.545	0.056	0.064	1.47	36.70	160	240	182
		0.583	0.112	0.524	0.058	0.066	1.58	39.50			190.4
		0.702	0.135	0.541	0.070	0.080	2.29	57.27			183.6
		0.546	0.105	0.570	0.054	0.063	1.39	34.64			172
600	1.082	0.928	0.178	0.510	0.078	0.089	4.31	107.81	240	360	294
		0.788	0.151	0.545	0.066	0.076	3.11	77.73			273
		0.620	0.119	0.510	0.052	0.059	1.92	48.12			294
		0.960	0.184	0.521	0.081	0.092	4.61	115.37			287.4
		0.876	0.168	0.531	0.074	0.085	3.84	96.07			281.4
800	1.062	0.751	0.144	0.541	0.056	0.064	2.93	73.36	320	480	367.2
		0.739	0.142	0.547	0.055	0.063	2.84	71.04			362.4
		0.713	0.137	0.493	0.053	0.059	2.65	66.13			405.6
		0.713	0.137	0.518	0.053	0.060	2.65	66.13			385.6
		0.792	0.152	0.503	0.059	0.066	3.26	81.59			397.6
		0.823	0.158	0.545	0.061	0.070	3.52	88.10			364
1000	1.049	0.644	0.124	0.493	0.043	0.048	2.21	55.22	400	600	507
		0.843	0.162	0.468	0.057	0.062	3.78	94.62			532
		0.791	0.152	0.477	0.053	0.059	3.33	83.31			523
		0.815	0.156	0.475	0.055	0.060	3.54	88.44			525
		0.823	0.158	0.476	0.055	0.061	3.61	90.18			524
		0.782	0.150	0.511	0.053	0.060	3.26	81.42			489

5. Conclusions

This work presents a study of T-stress at the crack tip of concrete specimens submitted to three-point bending and compact tension. Its effect on mode-I fracture is considered in terms of its relative value to the SIF at the crack tip, i.e. $B\alpha$. The expressions given in Eq. (16) for TPB and Eq. (20) for CT show that $B\alpha$ depends on the specimen's geometry as well as on the material's property. For TPB, T-stress tends to be zero when the relative crack length β is around 0.4, meaning that there is no influence on mode-I fracture at all. When T-stress is too small compared with SIF (i.e., $B\alpha$ is less than 0.375, including the fact that $B\alpha$ is negative), the advancing crack tip will stay on its original crack plane and the critical stress intensity factor thus determined is the true fracture toughness of mode-I fracture. The same conclusion can be extended to CT specimens, even though T-stress in CT specimens is always positive. For the regular size of TPB or CT specimens used in the laboratory to determine concrete fracture toughness based on the modified MTS, T-stress generally satisfies the condition $B\alpha < 0.375$, thus no influence is expected for mode-I fracture of concrete. The other important thing we must take care of is the choice of the specimen's size, because it significantly affects the K-dominance zone ahead of the crack tip.

From this study we can draw the conclusion that after the careful choice of the specimen's size, the influence of T-stress on mode-I fracture of concrete can be neglected. Probably one reason is that T-stress, which is parallel stress component at the crack tip, has limited contribution to the opening pattern of mode-I fracture, which is supposed to be perpendicular to the crack plane. If so, T-stress is supposed to affect significantly mode-II fracture of concrete, which will be further explored in our next study.

Abbreviations

ASTM American Society for Testing and Materials
CT compact tension
DKFM double-K fracture model
ECM effective crack model
FPZ fracture process zone

LEFM	linear elastic fracture mechanics
MTS	maximum tangential stress
RILEM	Union of Laboratories and Experts in Construction Materials, Systems and Structures
SIF	stress intensity factor
TPB	three point bending
TPFM	two parameter fracture model

Acknowledgements

The authors gratefully acknowledge the supports from the National Natural Science Foundation of China (Grant No. 51108055) and the Creative Research Groups of the National Natural Science Foundation of China (Grant No. 51121005).

References

[1] M.L. Williams, On the stress distribution at the base of a stationary crack, ASME J. Appl. Mech. 24 (1957) 109–114.
[2] F. Erdogan, G.C. Sih, On the crack extension in plates under plane loading and transverse shear, J. Basic Eng. 85 (5) (1963) 19–27.
[3] G.C. Sih, Strain-energy-density factor applied to mixed mode crack problems, Int. J. Fract. 10 (3) (1974) 305–321.
[4] X.M. Kong, N. Schluter, W. Dahl, Effect of triaxial stress on mixed-mode fracture, Eng. Fract. Mech. 52 (2) (1995) 379–388.
[5] J. Williams, P.D. Ewing, Fracture under complex stress – the angled crack problem, Int. J. Fract. 8 (4) (1972) 441–446.
[6] K. Sedighiani, J. Mosayebnejad, H. Ehsasi, H.R. Sahraei, The effect of T-stress on the brittle fracture under mixed mode loading, Eng. Fract. Mech. 10 (2011) 774–779.
[7] Y. Ueda, K. Ikeda, T. Yao, M. Aoki, Characteristics of brittle fracture under general combined modes including those under bi-axial tensile loads, Eng. Fract. Mech. 18 (1983) 1131–1158.
[8] D.G. Smith, M.R. Ayatollahi, M.J. Pavier, The role of T-stress in brittle fracture for linear elastic materials under mixed-mode loading, Fatigue Fract. Eng. Mater. Struct. 24 (2001) 137–150.
[9] M.R. Ayatollahi, M.R.M. Aliha, Cracked Brazilian disc specimen subjected to mode II deformation, Eng. Fract. Mech. 72 (2005) 493–503.
[10] T. Fett, D. Munz, T-stress and crack path stability of DCDC specimens, Int. J. Fract. 124 (2003) L165–L170.
[11] B. Cotterell, J.R. Rice, Slightly curved or kinked cracks, Int. J. Fract. 16 (1980) 155–169.
[12] M. Hadj Meliani, Y.G. Matvienko, G. Pluvinage, Two-parameter fracture criterion ($K_{\rho,c}$–$T_{ef,c}$) based on notch fracture mechanics, Int. J. Fract. 167 (2011) 173–182.
[13] M.R. Ayatollahi, K. Sedighiani, A T-stress controlled specimen for mixed mode fracture experiments on brittle materials, Eur. J. Mech. A, Solids 36 (2012) 83–93.
[14] M.F. Kaplan, Crack propagation and the fracture of concrete, J. Am. Concr. Inst. 58 (5) (1961) 591–610.
[15] F. Dubois, R. Moutou Pitti, B. Picoux, C. Petit, Finite element model for crack growth process in concrete bituminous, Adv. Eng. Softw. 44 (2012) 35–43.
[16] P.S. Leevers, J.C. Radon, Inherent stress biaxiality in various fracture specimen geometries, Int. J. Fract. 19 (1982) 311–325.
[17] M.R. Ayatollahi, M.J. Pavier, D.J. Smith, Mode I cracks subjected to large T-stresses, Int. J. Fract. 117 (2002) 159–174.
[18] G.V. Guinea, J. Pastor, J. Planas, M. Elices, Stress intensity factor, compliance and CMOD for a general three-point-bend beam, Int. J. Fract. 89 (1998) 103–116.
[19] B.L. Karihaloo, Q.Z. Xiao, Higher order terms of the crack tip asymptotic field for a notched three-point bend beam, Int. J. Fract. 112 (2001) 111–128.
[20] D. Taylor, M. Merlo, R. Pegley, M.P. Cavatorta, The effect of stress concentrations on the fracture strength of polymethylmethacrylate, Mater. Sci. Eng. A 382 (2004) 288–294.
[21] R.A. Schmidt, A microcrack model and its significance to hydraulic fracturing and fracture toughness testing, in: Proceedings of 21st US Symposium on Rock Mechanics, Rolla, MS, USA, 1980, pp. 581–590.
[22] Z.P. Bažant, Z.Z. Li, Modulus of rupture: size effect due to fracture initiation in boundary layer, J. Struct. Eng. 121 (4) (1995) 739–746.
[23] ASTM E399 $12^{\varepsilon 1}$, standard test method for linear-elastic plane-strain fracture toughness K_{IC} of metallic materials, ASTM International, PA, USA, 2013.
[24] K. Wallin, A simple fracture mechanical interpretation of size effects in concrete fracture toughness tests, Eng. Fract. Mech. 99 (2013) 18–29.
[25] Y.S. Jenq, S.P. Shah, Two-parameter fracture model for concrete, J. Eng. Mech. ASCE 111 (10) (1985) 1227–1241.
[26] B.L. Karihaloo, P. Nallathambi, Effective crack model for the determination of fracture toughness K_{Ic}^{s} of concrete, Eng. Fract. Mech. 35 (4–5) (1990) 637–645.
[27] S.L. Xu, H.W. Reinhardt, Determination of double-K criterion for crack propagation in quasi-brittle fracture. Part I: experimental investigation of crack propagation, Int. J. Fract. 98 (1999) 111–149.
[28] M. de Moura, J.J.L. Morais, N. Dourado, A new data reduction scheme for mode I wood fracture characterization using the double cantilever beam test, Eng. Fract. Mech. 75 (2008) 3852–3865.
[29] M. de Moura, N. Dourado, J. Morais, Crack equivalent based method applied to wood fracture characterization using the single edge notched-three point bending test, Eng. Fract. Mech. 77 (2010) 510–520.
[30] R.P. Ojdrovic, H.J. Petroski, Fracture behavior of notched concrete cylinder, J. Eng. Mech. ASCE 113 (12) (1987) 1551–1564.
[31] F. Xu, Z.M. Wu, J.J. Zheng, Y.H. Zhao, K. Liu, Crack extension resistance curve of concrete considering variation of FPZ length, J. Mater. Civ. Eng. ASCE 23 (5) (2011) 703–710.
[32] L.B. Qing, Q.B. Li, A theoretical method for determining initiation toughness based on experimental peak load, Eng. Fract. Mech. 99 (2013) 295–305.
[33] DL/T 5332-2005, specification for fracture test of hydraulic concrete, China Electric Power Press, Beijing, 2005.
[34] S.L. Xu, H.W. Reinhardt, Determination of double-K criterion for crack propagation in quasi-brittle materials. Part II: analytical evaluating and practical measuring methods for three-point bending notched beams, Int. J. Fract. 98 (1999) 151–177.
[35] Y.S. Jenq, S.P. Shah, A fracture toughness criterion for concrete, Eng. Fract. Mech. 21 (5) (1985) 1055–1069.
[36] Y.H. Zhao, The analytical study on the energy in the fracture process of concrete, doctoral dissertation, Dalian University of Technology, Dalian, China, 2002 (in Chinese).
[37] T. Fett, Stress Intensity Factors, T-Stresses, Weight Functions, Institute of Ceramics in Mechanical Engineering, University of Karlsruhe, Karlsruhe, Germany, 2008.
[38] S.L. Xu, D. Bu, X.F. Zhang, A study on double-K fracture parameters by using wedge-splitting test on compact tension specimens of various sizes, China Civ. Eng. J. 41 (2) (2008) 70–76 (in Chinese).